IBRACON

Volume 3, Number 2 (June 2007) p. 151-176 ISSN 1809-1121

Revista IBRACON de Estruturas

IBRACON Structural Journal

Anchor Bolts under Tension Loads – Influence of Casting Position and Edge Distance

Pinos de Ancoragens Sob Cargas de Tração – Influência da Posição e Proximidade da Borda



M. T. R. MEIRA [a]
magnus_meira@civ.puc-rio.br

R. B. GOMES [b]
rgomes@eec.ufg.br

G. B. GUIMARÃES [c]
giuseppe@civ.puc-rio.br

Abstract

A series of 51 square headed anchor bars was tested in axial tension, in which the main variables were bonded length along the bar, distance of the embedment to an edge, effective depth, casting position (top, middle and bottom) and orientation (horizontal and vertical) of the embedment in the concrete block. Test results showed that the anchor strength decreases linearly with the decrease of the distance of the embedment to an edge, and that the anchor strength can increase 2.6 times when the effective depth increases from 50 to 100 mm for top and bottom bars. The increase in the anchor strength due to bond ranged from 3% to 50%. It was observed that the ultimate strength of anchor located at the bottom can be 32% higher than that of anchor located at the top, and that orientation of the anchor did not affect the failure load.

Keywords: Anchor bolt, free edge influence, bond, casting position, embedment orientation.

Resumo

Neste trabalho foram testados 51 pinos de ancoragem curtos com cabeça quadrada, sujeitos a forças de tração, tendo como principais variáveis a distância do pino à borda, a altura efetiva, a existência de aderência ao longo da haste, a posição (superior, intermediário e inferior) e a orientação (horizontal e vertical) do pino no bloco de concreto. É demonstrado que a resistência da ancoragem diminui linearmente com a diminuição da distância até a borda e que com o aumento da altura efetiva, de 50 mm para 100 mm, a carga de ruptura pode aumentar 2,6 vezes nas ancoragens localizadas na posição inferior e superior do bloco. O aumento na carga última decorrente da aderência ao longo da haste do pino varia de 3% a 50 %. É observado que a resistência das ancoragens inferiores chega a ser 32% maior do que as superiores e que não há variação na carga de ruptura com a mudança na orientação.

Palavras-chave: Pino de ancoragem, influência de borda, aderência, posição, orientação.

[a] *Ph.D student, Departamento de Engenharia Civil, Pontifícia Universidade Católica do Rio de Janeiro, magnus_meira@civ.puc-rio.br, Rua Diunísio Filgueira, 780, Apto. 401 – Petrópolis – CEP 59014-020, Natal, Brasil;*
[b] *Full Professor, Escola de Engenharia Civil, Universidade Federal de Goiás, rgomes@eec.ufg.br, Praça Universitária, s/nº – Setor Universitário – CEP 74605-220, Goiânia, Brasil;*
[c] *Associate Professor, Departamento de Engenharia Civil, Pontifícia Universidade Católica do Rio de Janeiro, giuseppe@civ.puc-rio.br, Rua Marquês de São Vicente, 225 – Gávea – CEP 22453-900, Rio de Janeiro, Brasil.*

1 Introduction

Headed anchor bars have been used in structures such as hydroelectric and nuclear power plants where heavy equipments and pipelines are supported by concrete members. Their primary function is to fix the equipments and piping, introducing concentrated loads on the concrete members. The anchor studied in the present work is formed by a square plate welded at the end of a straight reinforcing deformed bar. This type of anchorage was first developed for use in joints of framed concrete structures of offshore platforms [1].
The objective of the present work was to study the strength of a shallow embedment anchor bar failing by concrete cone breakout, throughout a series of 51 pull-out tests. The main variables were bonded length along the bar, embedment distance to an edge, effective depth, casting position (top, middle and bottom of the concrete block) and orientation (horizontal and vertical) of the embedment inside the block.

1.1 Variables affecting the ultimate capacity

The variables that affect the ultimate capacity of shallow embedment anchor bar failing by concrete cone breakout are concrete strength, bonded length along the bar (only for reinforcing deformed bar), edge distance, effective depth, head size, casting position and embedment orientation.
The concrete cone breakout mode of failure clearly indicates that the ultimate capacity depends on the concrete tensile strength. Bond along the embedment length improves the slip performance of the anchor and provides a small increase in ultimate capacity [2].
The behavior of anchor systems close to an edge is similar to the behavior of anchor systems in cracked zones. According to Eligehausen *et al.* [3], cracks affect the ultimate capacity because they create a stress disturbance zone which causes a decrease of the surface area available to transfer tension forces and do not allow axi-symmetric force transference (Figure 1).
The concrete cone failure load increases with the increase of the embedment depth h_{ef}. Assuming no size-effect, the failure load increases in proportion to h_{ef}^2. Studies based on fracture mechanics (Eligehausen e Ozbolt [4]) have shown that the failure load is affected by a factor of $h_{ef}^{-0.5}$, resulting in a failure load proportional to $h_{ef}^{1.5}$. According to Ozbolt *et al.* [5], when the head size increases the ductility of the response decreases, but the concrete breakout resistance increases.
Casting position refers to the location of the bar within the fresh concrete and orientation refers to the direction of the bar relative to the direction of concrete casting. Luke *et al.* [6] observed that the bond strength of embedded deformed bars cast near the edge decreased with the increase in the depth of concrete cast below the bar and that vertical bars (parallel to the direction of concrete casting) displayed less bond capacity than horizontal bars at the same level.

2 Experimental program and materials

2.1 Experimental program

Compressive concrete strength f_c, bar diameter d and head size d_h were kept constant. The variables adopted in this work are described below.

- Edge distance c_x: distance from the bar axis to the closest edge (Figure 2a);
- Effective embedment depth h_{ef}: distance from the top (loaded) surface of the test specimen to the inner surface of the head (Figure 2a);

Figure 1 – Load transfer mechanism example (Eligehausen et al. (3))

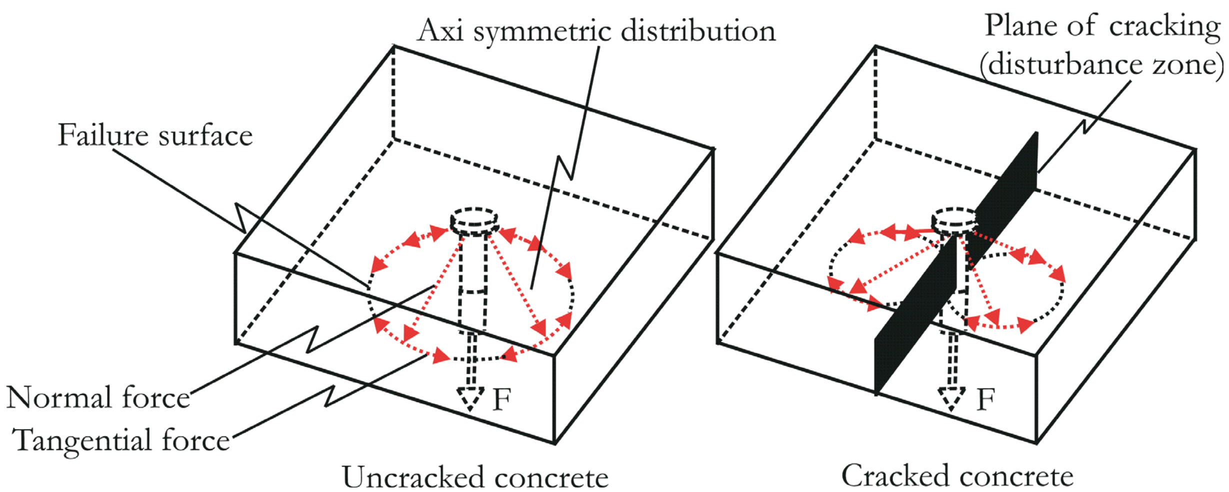

Figure 2 – (a) Geometrical characteristics; (b) Anchor casting position and orientation

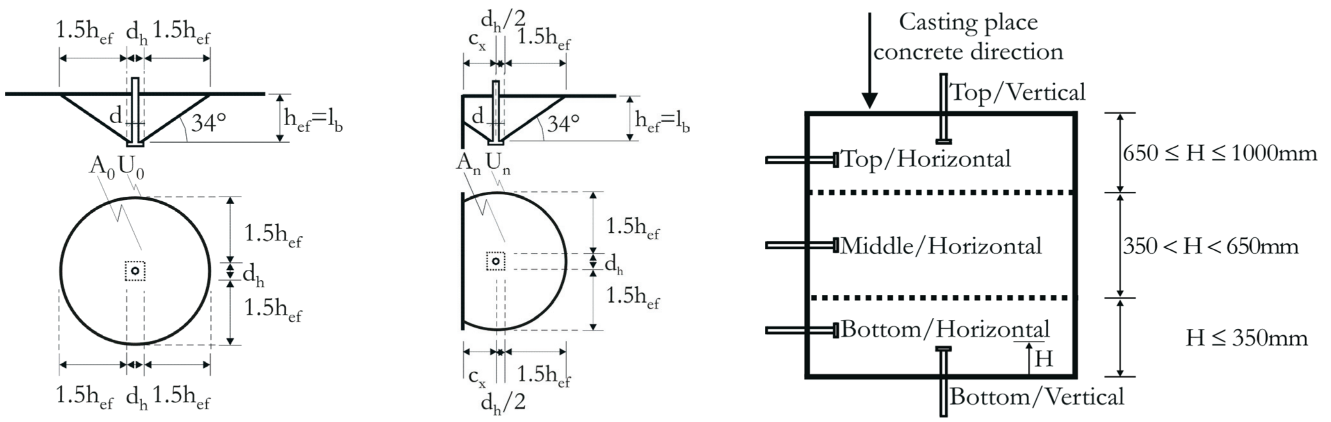

(a) Geometrical characteristics

(b) Anchor casting position and orientation

- Bonded length l_b : length along which bond exist between concrete and bar (Figure 2a);
- Casting position: position of the anchor at the occasion of casting, relative to the height of the concrete block; three positions were considered: top, middle and bottom (Figure 2b);
- Orientation: direction, horizontal or vertical, of bar axis (Figure 2b).

Depending on the edge distance, two additional dependent variables were obtained: the ratio of the projected area A_n, limited by the edge, of the concrete cone at the concrete surface to the total projected area A_o and the ratio of the perimeter U_n of A_n to the perimeter U_0 of A_o. The radius of both areas is $1.5h_{ef} + d_h/2$ (Figure 2 a).

Four concrete blocks with dimensions 1000 x 1000 x 1000 mm were constructed for the tests. In each block, the headed bars were spaced at distances sufficient to avoid overlap of the failure cones. The distance between the supports of the frame (Figure 3), was higher than six times the embedment depth in order to avoid any interference of the frame reactions on the concrete cone.

Figure 3 – Test setup (measures in mm)

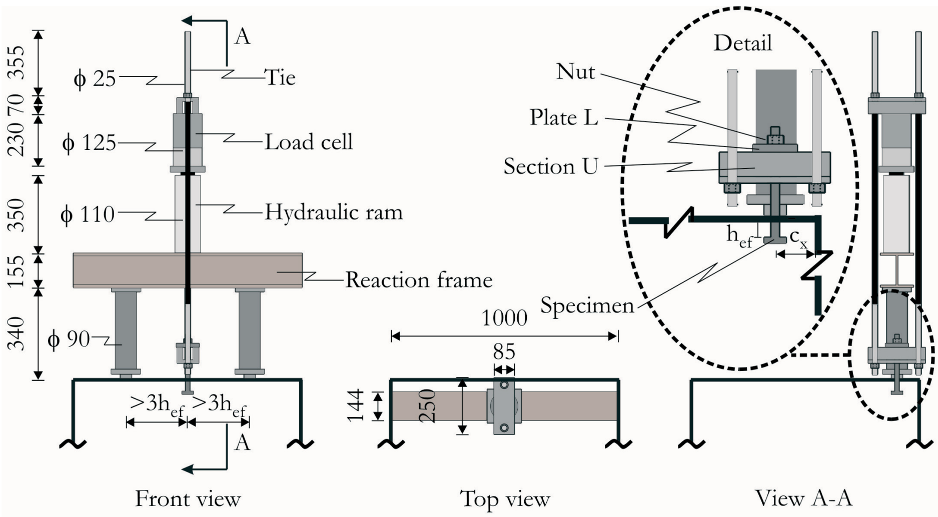

Axial displacement of the anchor relative to a point outside the failure cone was measured by a dial gage. This displacement includes the elongation of the bar and the head displacement due to concrete deformation. The load was applied in small increments and was measured with a load cell.

2.2 Materials

The bars were made of CA-50 steel (specified yield strength of 500 MPa) with diameter of 20 mm. Their mechanical properties were obtained by tests carried out on two samples according to NBR6152/92 [7]. The values of yield and ultimate strength were 570 MPa and 677 MPa respectively. The elastic modulus was 211 GPa and the strain corresponding to yield strength was 2.7 mm/m.
The target compressive strength of concrete was 20 MPa at 28 days. Aggregate maximum-size was 19 mm and the specified slump was 90 mm ± 10 mm. Concrete cylinders 150 x 300 mm were cast to obtain the compressive strength [8], elastic modulus [9] and the splitting tensile strength [10] at 28 days. The values obtained for the concrete used in blocks 1 and 2 and blocks 3 and 4 were: 19.7 and 20.3 MPa for the compressive strength; 2.43 and 2.50 MPa for the tensile strength and 21.6 and 22.6 GPa for the elastic modulus.

3 Results and discussion

3.1 Failure modes and ultimate loads

The mode of failure of all specimens was pullout cone failure delimitated by a surface initiating at the head of the anchor and progressing towards the block surface, as shown in Figure 4. In some cases, cracks appeared in the region around the head indicating the beginning of lateral failure and/or cracks that splitted the concrete cone into a number of blocks, as shown in Figure 5.
The ultimate load and mode of failure of the anchor bars with effective depth of 50 mm and 100 mm are shown in Tables 1 and 2 together with bonded length, casting position and orientation, compressive and tensile concrete strengths f_c and f_t, and the measured ratios A_n/A_0, U_n/U_0 and c_x/h_{ef}.

3.2 Influence of bonded length

The comparison of the ultimate loads $F_{u,bond}$ of the anchor with bonded length l_b equal to effective depth h_{ef} with the ultimate loads $F_{u,no\ bond}$ of the anchor without bond is shown in Table 3. It is observed that all values of the

Figure 4 – Inferior, lateral and perspective views of observed concrete breakout cones (measures in mm)

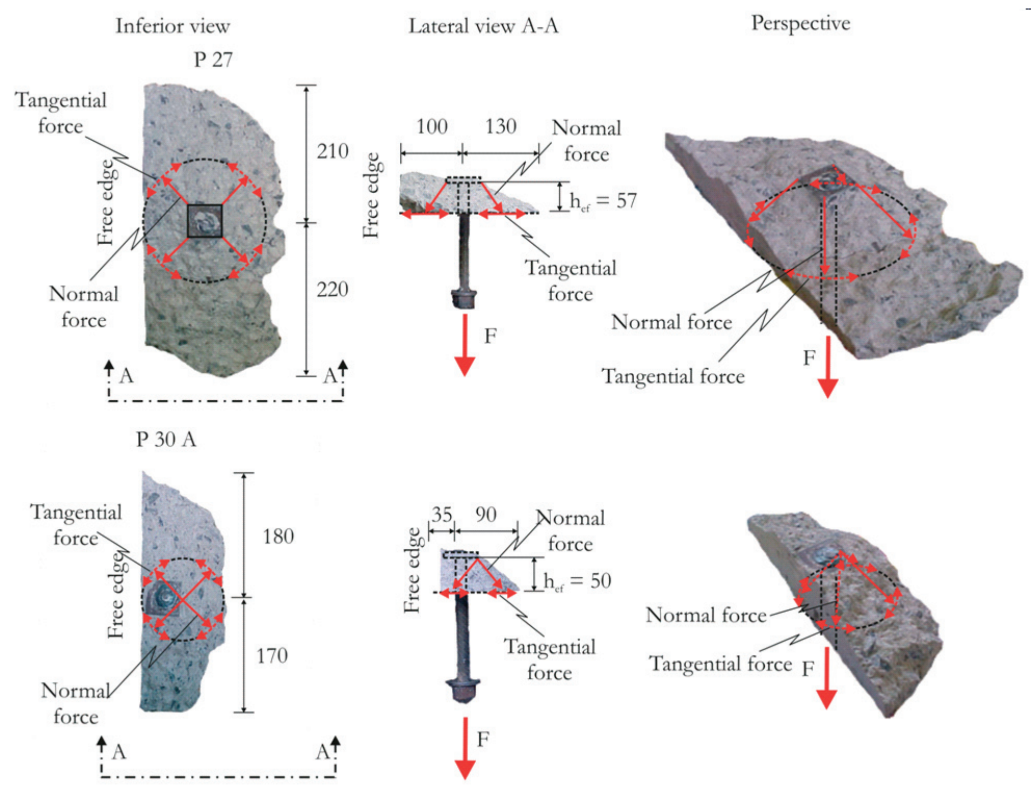

Figure 5 – Inferior, lateral and perspective views of concrete cones with splitting cracks or side circular cracks near to head (measures in mm)

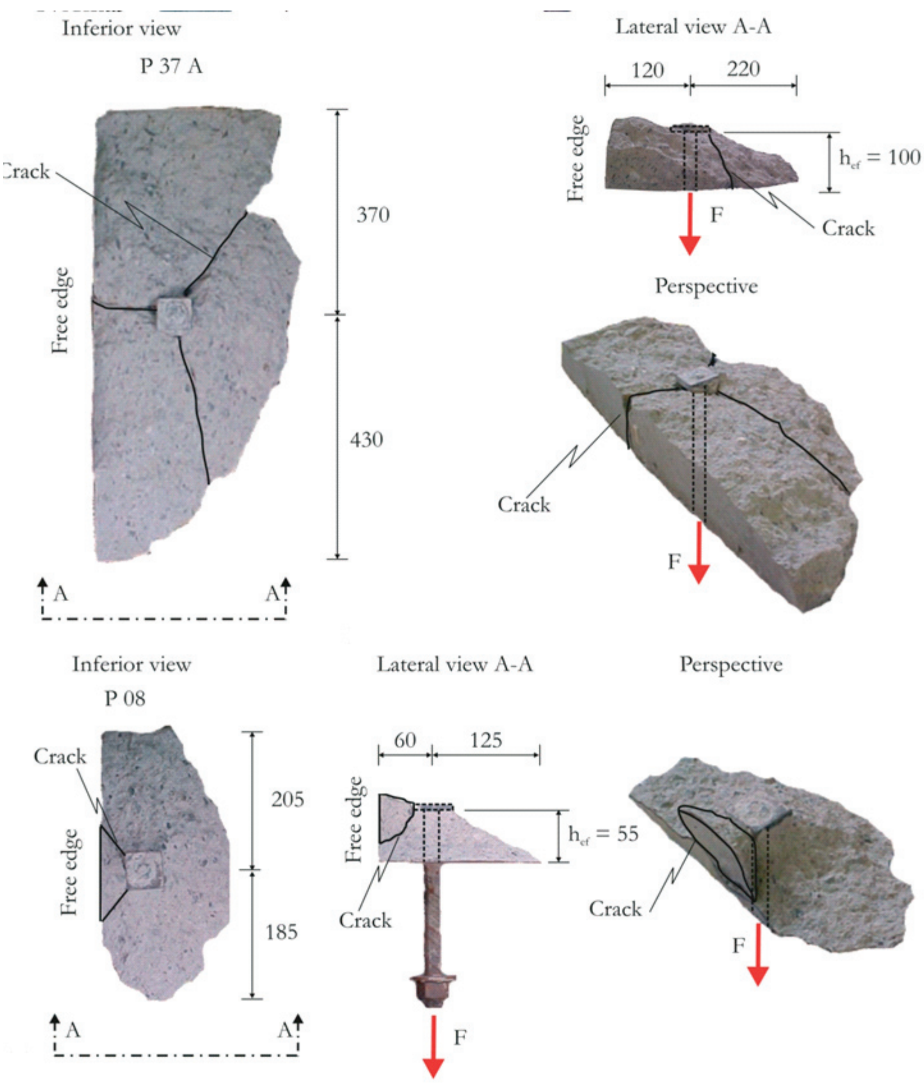

$F_{u,bond}/F_{u,no\ bond}$ ratio were higher than 1.0. This can be explained by the reduction of the stress exerted by the head of the anchor on the concrete caused by bond stress developed along the bonded length [2].
The mean value of the $F_{u,bond}/F_{u,no\ bond}$ ratio varied from 1.21 (for top anchor with $h_{ef} = 50$ mm and bottom anchor with $h_{ef} = 100$ mm) to 1.43 (middle anchors with $h_{ef} = 50$ mm). The mean value of the increase of the anchorage capacity for the anchors with $l_b = h_{ef}$ was 32.0%, with coefficient of variation of 18.5%.

3.3 Influence of edge distance

To estimate the loss of the anchor strength due to a close edge, the ratio of the ultimate load $F_{u,n}$ of each anchor to the ultimate load $F_{u,Iso}$ of the isolated anchor ($F_{u,n}/F_{u,Iso}$) was calculated (Table 4). The anchors with effective depth of 50 mm, at the top position and orientated vertically, presented decreasing values of $F_{u,n}/F_{u,Iso}$ from 1.00 to 0.53 for $A_n/A_0 = 1.00$ and $A_n/A_0 = 0.70$ respectively. This reduction was also observed for the other situations.
The anchors with 100 mm effective depth, located at the middle position and orientated horizontally, presented the lowest values of $F_{u,n}/F_{u,Iso}$ because the concrete in the block corners could be of poorer quality.

Table 1 – Ultimate load and failure mode of the anchors with effective depth of 50 mm

Casting position	l_b (mm)	Orientation	A_n/A_0 U_n/U_0 c_x/h_{ef}	1.00 1.00 10.00 (Isolated)	A_n/A_0 U_n/U_0 c_x/h_{ef}	1.00 1.00 2.00	A_n/A_0 U_n/U_0 c_x/h_{ef}	0.90 0.75 1.40	A_n/A_0 U_n/U_0 c_x/h_{ef}	0.80 0.68 1.04	A_n/A_0 U_n/U_0 c_x/h_{ef}	0.70 0.61 0.70
Top	50	Horizontal	**P** Block $h_{ef}^{mea.}$ $A_n/A_0^{mea.}$ f_c	**F_u (kN)** F. M. $c_x/h_{ef}^{mea.}$ $U_n/U_0^{mea.}$ f_t	**P01** 1 52 1.00 19.70	**29.5** cc 1.92 0.92 2.43	**P02** 1 52 0.89 19.70	**21.6** cc/s 1.35 0.74 2.43	**P03A** 3 53 0.81 20.30	**21.5** cc/s 1.04 0.68 2.50	**P04** 1 50 0.74 19.70	**16.4** cc 0.84 0.64 2.43
Top	50	Vertical	**P05** 2 55 1.00 19.70	**32.0** cc 9.09 1.00 2.43	**P06** 1 55 1.00 19.70	**28.4** cc 1.91 0.93 2.43	**P07** 1 50 0.87 19.70	**22.4** cc 1.30 0.73 2.43	**P08B** 3 55 0.80 19.20	**23.0** cc/scc 1.00 0.67 2.36	**P09B** 3 50 0.70 19.50	**17.0** cc/scc 0.70 0.61 2.40
Top	0	Horizontal	- - - - -	- - - - -	**P10** 3 50 1.00 20.30	**21.3** cc 2.00 1.00 2.50	**P11** 3 50 0.90 20.30	**20.1** cc 1.40 0.75 2.50	- - - - -	- - - - -	**P12** 3 50 0.73 20.30	**14.0** cc/scc 0.80 0.63 2.50
Middle	50	Horizontal	**P13** 2 50 1.00 19.70	**34.1** cc 10.00 1.00 2.43	**P14** 1 50 1.00 19.70	**32.3** cc 2.00 1.00 2.43	**P15A** 3 52 0.91 20.30	**27.8** cc 1.44 0.76 2.50	**P16** 1 49 0.80 19.70	**24.0** cc 1.02 0.67 2.43	**P17** 1 52 0.69 19.70	**19.9** cc 0.65 0.61 2.43
Middle	0	Horizontal	**P18** 4 50 1.00 20.30	**26.6** cc 10.00 1.00 2.50	**P19** 3 55 1.00 20.30	**31.4** cc 1.91 0.93 2.50	- - - - -	- - - - -	**P20** 3 50 0.79 20.30	**12.5** cc 1.00 0.67 2.50	**P21** 3 53 0.72 20.30	**13.2** cc 0.75 0.62 2.50
Bottom	50	Horizontal	- - - - -	- - - - -	**P22** 1 50 1.00 19.70	**37.0** cc/s 2.10 1.00 2.43	**P23** 1 55 0.86 19.70	**33.0** cc 1.22 0.71 2.43	**P24** 1 55 0.80 19.70	**26.8** cc 1.00 0.67 2.43	**P25** 1 50 0.74 19.70	**22.1** cc 0.84 0.64 2.43
Bottom	50	Vertical	**P26** 2 52 1.00 19.70	**39.1** cc 9.62 1.00 2.43	**P27** 1 57 0.98 19.70	**40.6** cc 1.75 0.86 2.43	**P28** 1 50 0.90 19.70	**32.7** cc/s 1.40 0.75 2.43	**P29** 1 50 0.85 19.70	**24.8** cc/s 1.10 0.70 2.43	**P30A** 3 50 0.70 20.30	**22.4** cc 0.70 0.61 2.50
Bottom	0	Horizontal	- - - - -	- - - - -	**P31** 3 50 1.00 20.30	**24.7** cc 2.05 1.00 2.50	**P32** 3 50 0.87 20.30	**24.4** cc 1.30 0.73 2.50	**P33** 3 54 0.80 20.30	**24.6** cc 1.02 0.67 2.50	**P34** 3 55 0.72 20.30	**16.0** cc/s/scc 0.73 0.62 2.50

l_b - Bond length.
P - Specimen identification.
h_{ef} e $h_{ef}^{mea.}$ - Effective depth (hef) required and measured.
c_x/h_{ef} e $c_x/h_{ef}^{mea.}$ - Relation between the free edge distance (c_x) and the effective depth (h_{ef}) required and measured.
A_n/A_0 e $A_n/A_0^{mea.}$ - Relation between required and measured assumed total projected concrete failure area (A_0) and partial (A_n).
U_n/U_0 e $U_n/U_0^{mea.}$ - Relation between required and measured perimeter of assumed total projected concrete failure area (U_0) and partial (U_n)
F_u - Failure load.
F. M. - Failure mode.
cc - Pullout cone failure (cc).
cc/scc - Pullout concrete cone failure (cc) with side circular cracks near to head (scc).
cc/s - Pullout concrete cone failure (cc) with splitting cracks (s).
cc/s/scc - Pullout concrete cone failure (cc) with splitting cracks (s) and side circular cracks near to head (scc).

3.4 Influence of effective depth

The ultimate loads $F_{u,100}$ and $F_{u,50}$ of the anchors with 100 mm and 50 mm effective depth are compared in Table 5 for the anchors at the same position, orientation and A_n/A_0 ratio. The mean values of $F_{u,100}/F_{u,50}$ and of the coefficient of variation of the anchors located at the top and bottom positions show little differences; if they are considered altogether, these values would be 2.62 e 0.08 respectively.

The anchors located at the middle position showed the lowest values for the ratio $F_{u,100}/F_{u,50}$ due to the higher strength loss of the anchors with 100 mm effective depth close to an edge. The mean value of $F_{u,100}/F_{u,50}$ was 2.29 and the coefficient of variation was 0.23.

3.5 Influence of casting position

The influence of casting position is verified by comparing the values of the ultimate loads of the anchors located at bottom ($F_{u,bot}$) and middle ($F_{u,mid}$) positions and the ultimate loads ($F_{u,top}$) of the anchors located at the top position, as shown in Table 6. In general, the bottom and middle anchors displayed ultimate loads higher than those of the top anchors.

The mean values of the ultimate loads of the bottom and

Table 2 – Ultimate load and failure mode of the anchors with effective depth of 100 mm

Casting position	l_b (mm)	Orientation	A_n/A_0 U_n/U_0 c_x/h_{ef}	1.00 1.00 5.00	A_n/A_0 U_n/U_0 c_x/h_{ef}	1.00 1.00 1.75	A_n/A_0 U_n/U_0 c_x/h_{ef}	0.90 0.75 1.21	A_n/A_0 U_n/U_0 c_x/h_{ef}	0.80 0.68 0.88	A_n/A_0 U_n/U_0 c_x/h_{ef}	0.70 0.61 0.58
			Isolated									
Top	100	Vertical	**P35** 1 100 1.00 19.70	**77.9** cc 5.00 1.00 2.43	**P36A** 4 100 1.00 19.00	**67.9** cc/s 1.80 1.00 2.34	**P37A** 4 100 0.90 18.90	**65.6** cc/s 1.20 0.74 2.33	**P38** 2 107 0.78 19.70	**61.9** cc 0.79 0.65 2.43	**P39** 2 110 0.69 19.70	**43.9** cc 0.53 0.60 2.43
Middle	100	Horizontal	**P40** 2 102 1.00 19.70	**102.6** cc/s 4.90 1.00 2.43	**P41** 2 103 1.00 19.70	**85.4** cc 1.75 1.00 2.43	**P42A** 4 100 0.91 20.30	**52.8** cc 1.25 0.75 2.50	**P43A** 4 100 0.79 20.30	**50.4** cc/s 0.85 0.66 2.50	**P44A** 4 100 0.67 20.30	**35.6** cc 0.50 0.59 2.50
Bottom	100	Vertical	**P45** 1 105 1.00 19.70	**108.7** cc/s 4.76 1.00 2.43	**P46** 2 103 1.00 19.70	**99.2** cc/s 1.75 1.00 2.43	**P47** 2 102 0.89 19.70	**77.6** cc/s 1.18 0.74 2.43	**P48** 2 105 0.81 19.70	**71.9** cc 0.90 0.67 2.43	**P49** 2 105 0.69 19.70	**60.9** cc 0.55 0.60 2.43
Bottom	0	Vertical	**P** Block $h_{ef}^{mea.}$ $A_n/A_0^{mea.}$ f_c	**F_u (kN)** F. M. $c_x/h_{ef}^{mea.}$ $U_n/U_0^{mea.}$ f_t	**P50** - - - -	**-** - - - -	**P51** 4 95 0.91 20.30	**71.0** cc/s 1.26 0.75 2.50	**P52** - - - -	**-** - - - -	**P53** 4 105 0.68 20.30	**45.9** cc 0.52 0.60 2.50

l_b - Bond length.
P - Specimen identification.
h_{ef} e $h_{ef}^{mea.}$ - Effective depth (hef) required and measured.
c_x/h_{ef} e $c_x/h_{ef}^{mea.}$ - Relation between the free edge distance (c_x) and the effective depth (h_{ef}) required and measured.
A_n/A_0 e $A_n/A_0^{mea.}$ - Relation between required and measured assumed total projected concrete failure area (A_0) and partial (A_n).
U_n/U_0 e $U_n/U_0^{mea.}$ - Relation between required and measured perimeter of assumed total projected concrete failure area (U_0) and partial (U_n)
F_u - Failure load.
F. M. - Failure mode.
cc - Pullout cone failure (cc).
cc/scc - Pullout concrete cone failure (cc) with side circular cracks near to head (scc).
cc/s - Pullout concrete cone failure (cc) with splitting cracks (s).

middle anchors were 1.32 and 1.18, respectively, higher than the mean values of ultimate loads of the superior anchors. This increase is attributed to the better quality of concrete at the bottom of the concrete block, where there is a higher concentration of coarse aggregate, and due to the higher amount of concrete above the anchors.

3.6 Influence of orientation

Table 7 shows the ultimate loads of the group of anchors with horizontal and vertical orientations, located at the top and bottom positions in the concrete block. The ratio $F_{u,H.}/F_{u,V.}$ of the ultimate load $F_{u,H.}$ of a horizontal anchor to the ultimate load $F_{u,V.}$ of a vertical anchor presents little variation around the unit value, for the anchors located at both superior and inferior positions. The mean value of this ratio is 0.99 with coefficient of variation of 5.6%. These results show that the orientation of the anchor has no influence on the anchor strength for effective depth of 50 mm.

3.7 Displacements

The measured axial displacement Δl relative to the concrete block includes the elongation Δl^{c}_{steel} of the external length of the bar and the displacement δ due to the elongation of the embedded bar length plus the head displacement (Figure 6). Δl^{c}_{steel} can be evaluated (while the bar behaves linearly) by the expression Fl/EA (E = 210 GPa). For the anchors with bonded length ($l_b = h_{ef}$), the displacement $\delta = \Delta l - \Delta l^{c}_{steel}$ is due to the elongation of the embedded bar length plus the head displacement. For the anchors without bond ($l_b = 0$), δ is due to the head displacement only.
Figure 7 shows the load-displacement response of the anchors with effective depth of 50 mm and 100 mm, at the top, middle and bottom positions, and with A_n/A_0 = 0.90.
The anchors located at top position (P37A and P07) had the highest displacements δ, for each effective depth at the same percentage of ultimate load.
The increase of effective depth from 50 mm to 100 mm caused an increase of δ for the same percentage of ultimate load due to the decrease of the ratio of the head

Table 3 – Influence of bonded length

h_{ef} (mm)	Casting position	Orient.	A_n/A_0	Bond $l_b=h_{ef}$ Specimen	Bond $l_b=h_{ef}$ $F_{u,bond}$ (kN)	No bond $l_b=0$ Specimen	No bond $l_b=0$ $F_{u,no\ bond}$ (kN)	$F_{u,bond}/F_{u,no\ bond}$
50	Top	Horizont.	10	P01	29.5	P10	21.3	1.38
			0.9	P02	21.6	P11	20.1	1.07
			0.7	P04	16.4	P12	14.0	1.17
	Middle	Horizont.	Iso -1.0	P13	34.1	P18	26.6	1.28
			1.0	P14	32.3	P19	31.4	1.03
			0.8	P16	24.0	P20	12.5	1.92
			0.7	P17	19.9	P21	13.2	1.51
	Bottom	Horizont.	1.0	P22	37.0	P31	24.7	1.50
			0.9	P23	33.0	P32	24.4	1.35
			0.8	P24	26.8	P33	24.6	1.09
			0.7	P25	22.1	P34	16.0	1.38
100	Bottom	Vertical	0.9	P47	77.6	P51	71.0	1.09
			0.7	P49	60.9	P53	45.9	1.33

Value	$F_{u,bond}/F_{u,no\ bond}$ Top $h_{ef\ 50}$	Middle $h_{ef\ 50}$	Bottom $h_{ef\ 50}$	Bottom $h_{ef\ 100}$	All
Maximum	1.38	1.92	1.50	1.33	1.92
Minimum	1.07	1.03	1.09	1.09	1.03
Mean	1.21	1.43	1.33	1.21	1.32
Coeff. of variation (%)	13.1	26.4	13.0	13.7	18.5

size to the effective depth. Low values of this ratio cause a reduction of the effective depth due to concrete crushing above the head [5].
Figure 8 shows the load-displacement δ curves of the anchors with and without bond ($l_b = h_{ef}$ and $l_b = 0$) which have, for the each effective depth, same A_n/A_0 ratio, same position and orientation. For the anchors without bond, the displacement δ is relative to the head only.
The bonded anchors ($l_b = h_{ef}$), P22 and P47, showed the lowest displacements $\delta = \Delta l - \Delta l^c_{steel}$ as compared to the anchors with no bond ($l_b = 0$), because the ribs acted as an additional mechanical anchorage which provided the reduction of the displacements.

4 Conclusions

The objective of the present work was to study the strength of a shallow embedment anchor bar failing by concrete cone breakout, throughout a series of 51 pullout tests. The results presented in this study have shown that:
• the ultimate loads of bonded anchor bars were 3% to 50% higher than the ultimate loads of anchors with no bond, with mean value of 32% and corresponding coefficient of variation of 18.5%;
• the lower the distance to an edge, the lower the ultimate load of the anchorage; for the smallest distance consid-

Table 4 – Influence of edge distance

h_{ef} (mm)	Casting position	Orientation	Specimen	A_n/A_0	$F_{u,n}$ (kN)	$F_{u,n}/F_{u,Iso}$
50	Top	Vertical	P05	Iso-1.0	32.0	1.00
			P06	1.0	28.4	0.89
			P07	0.9	22.4	0.70
			P08B	0.8	23.0	0.72
			P09B	0.7	17.0	0.53
	Middle	Horizontal	P13	Iso-1.0	34.1	1.00
			P14	1.0	32.3	0.95
			P15A	0.9	27.8	0.82
			P16	0.8	24.0	0.70
			P17	0.7	19.9	0.58
	Bottom	Vertical	P26	Iso-1.0	39.1	1.00
			P27	1.0	40.6	1.04
			P28	0.9	32.7	0.84
			P29	0.8	24.8	0.63
			P30A	0.7	22.4	0.57
100	Top	Vertical	P35	Iso-1.0	77.9	1.00
			P36A	1.0	67.9	0.87
			P37A	0.9	65.6	0.84
			P38	0.8	61.9	0.79
			P39	0.7	43.9	0.56
	Middle	Horizontal	P40	Iso-1.0	102.6	1.00
			P41	1.0	85.4	0.83
			P42A	0.9	52.8	0.51
			P43A	0.8	50.4	0.49
			P44A	0.7	35.6	0.35
	Bottom	Vertical	P45	Iso-1.0	108.7	1.00
			P46	1.0	99.2	0.91
			P47	0.9	77.6	0.71
			P48	0.8	71.9	0.66
			P49	0.7	60.9	0.56

ered in this study, a reduction of 35% in relation to an isolated anchor was observed;
• the increase of effective depth from 50 mm to 100 mm resulted in an increase of the anchor capacity up to 2.29 times for anchors located at middle position and up to 2.62 times for the top and bottom anchors;
• ultimate loads of anchor bars located at bottom and middle positions were 32% and 18% higher than ultimate loads of top anchors;
• the orientation of the anchors had no effect on the anchor capacity of the anchors with effective depth of 50 mm;
• the displacement due to head displacement plus the elongation of the immersed bar length of the top anchors were higher than the displacements observed in the bottom and middle anchors;
• anchors with effective depth of 100 mm presented displacements higher than those observed in the anchors with effective depth of 50 mm at the same load level expressed as a percentage of the ultimate load;
• bond between bar and concrete reduces the head displacements.

5 Acknowledgments

The authors are grateful to CAPES (Brazilian research funding agency) for the financial support and to Carlos Campos Consultoria; Companhia Siderúrgica Belgo-Mineira; Furnas Centrais Elétricas S. A.; IMPERCIA – Produtos Químicos para Construção; Perfinasa – Perfilados e Ferros Nossa Senhora Aparecida Ltda; Presmetal – Indústria & Prestação de Serviço Metalúrgicos Ltda; and Realmix – Concreto e Argamassa for assistance and material support.

6 References

[01] THOMPSON, M. K.; JIRSA, J. O.; BREEN, J.E; KLINGNER, R.E. Anchorage Behavior of Headed Reinforcement: Literature Review, Research Report Nº1855-1, Center for Highway Research, The University of Texas at Austin, Texas, May 2002, 116 p.
[02] DE VRIES, R. A.; JIRSA, J. O.; BASHANDY, T. Anchorage Capacity in Concrete of Headed

Table 5 – Influence of effective depth

Casting position	Orientation	A_n/A_0	h_{ef} = 50 mm		h_{ef} = 100 mm		$F_{u,100}/F_{u,50}$
			Specimen	$F_{u,50}$ (kN)	Specimen	$F_{u,100}$ (kN)	
Top	Vertical	Iso -1.0	P05	32.0	P35	77.9	2.43
		1.0	P06	28.4	P36A	67.9	2.39
		0.9	P07	22.4	P37A	65.6	2.93
		0.8	P08B	23.0	P38	61.9	2.69
		0.7	P09B	17.0	P39	43.9	2.58
Middle	Horizontal	Iso -1.0	P13	34.1	P40	102.6	3.01
		1.0	P14	32.3	P41	85.4	2.64
		0.9	P15A	27.8	P42A	52.8	1.90
		0.8	P16	24.0	P43A	50.4	2.10
		0.7	P17	19.9	P44A	35.6	1.79
Bottom	Vertical	Iso -1.0	P26	39.1	P45	108.7	2.78
		1.0	P27	40.6	P46	99.2	2.44
		0.9	P28	32.7	P47	77.6	2.37
		0.8	P29	24.8	P48	71.9	2.90
		0.7	P30A	22.4	P49	60.9	2.72

Value	Fu,100/Fu,50			
	Top	Middle	Bottom	Top and Bottom
Maximum	2.93	3.01	2.90	2.93
Minimum	2.39	1.79	2.37	2.37
Mean	2.61	2.29	2.64	2.62
Coeff. of variation (%)	8.3	22.7	8.5	8.0

Reinforcement with Shallow Embedments, ACI Structural Journal, v. 96, n. 5, p. 728 – 736,Sep.-Oct. 1999.
[03] ELIGEHAUSEN, R.; FUCHS, W.; MAYER, B. Tragverhalten von Dübelbefestingungen bei Zugbeanspruchung Teil 2 (Bearing Behaviour of anchor fastenings Under Tension, Part 2), Betonwerk +Fertigteil–Technik, n. 1, p.29–35, 1988.
[04] ELIGEHAUSEN, R.; OZBOLT, J. Size effect in anchorage behavior, Proceedings of the 8th European Conference on Fracture – Fracture Behavior and Design of Materials and Structures, p. 2671– 2677, 1990.
[05] OZBOLT, J.; ELIGEHAUSEN, R. and REINHARDT, H. W. Size Effect on the Concrete Cone Pull-out Load, International Journal of Fracture, v. 95, p.391–404, 1999.
[06] LUKE, J .J.; HAMAD, B. S.; JIRSA, J.O.; BREEN, J.E. The Influence of Casting Position on Development and Splice Length of Reinforcing Bars, Research Report 242-1, Center for Highway Research, The University of Texas at Austin, Texas, June 1981, 174pp.
[07] ASSOCIAÇÃO BRASILEIRA DE NORMAS TÉCNICAS. Materiais metálicos – Determinação das propriedades mecânicas à tração. – NBR 6152/92, Rio de Janeiro, 1992.

Table 6 – Influence of casting position

h_{ef} (mm)	Orientation	A_n/A_0	Top Specimen	Top $F_{u,top}$ (kN)	Bottom Specimen	Bottom $F_{u,bot.}$ (kN)	$F_{u,bot.}/F_{u,top}$
50	Horizontal	1.0	P01	29.5	P22	37.0	1.25
		0.9	P02	21.6	P23	33.0	1.53
		0.8	P03A	21.5	P24	26.8	1.25
		0.7	P04	16.4	P25	22.1	1.35
	Vertical	Iso - 1.0	P05	32.0	P26	39.1	1.22
		1.0	P06	28.4	P27	40.6	1.43
		0.9	P07	22.4	P28	32.7	1.46
		0.8	P08B	23.0	P29	24.8	1.08
		0.7	P09B	17.0	P30A	22.4	1.32
100	Vertical	Iso - 1.0	P35	77.9	P45	108.7	1.40
		1.0	P36A	67.9	P46	99.2	1.46
		0.9	P37A	65.6	P47	77.6	1.18
		0.8	P38	61.9	P48	71.9	1.16
		0.7	P39	43.9	P49	60.9	1.39

h_{ef} (mm)	Orientation	A_n/A_0	Top Specimen	Top $F_{u,top}$ (kN)	Middle Specimen	Middle $F_{u,mid.}$ (kN)	$F_{u,mid.}/F_{u,top}$
50	Horizontal	1.0	P01	29.5	P14	32.3	1.09
		0.9	P02	21.6	P15A	27.8	1.29
		0.8	P03A	21.5	P16	24.0	1.12
		0.7	P04	16.4	P17	19.9	1.21

Value	$F_{u,bot.}/F_{u,top}$	$F_{u,mid.}/F_{u,top}$
Maximum	1.53	1.29
Minimum	1.08	1.09
Mean	1.32	1.18
Coeff. of variation (%)	10.0	7.6

[08] ASSOCIAÇÃO BRASILEIRA DE NORMAS TÉCNICAS. Ensaio de compressão de corpos de prova cilíndricos de concreto. – NBR 5739/94, Rio de Janeiro, 1994.
[09] ASSOCIAÇÃO BRASILEIRA DE NORMAS TÉCNICAS. Concreto – Determinação do módulo de deformação estática e diagrama tensão-deformação – Método e ensaio. – NBR 8522/84, Rio de Janeiro, 1984.
[10] ASSOCIAÇÃO BRASILEIRA DE NORMAS TÉCNICAS. Argamassa e Concreto – Determinação da resistência à tração por compressão diametral de corpos de prova cilíndricos – Método de ensaio. – NBR 7222/94, Rio de Janeiro, 1994.
[11] MEIRA, M. T. R. Resistência a Tração de Pinos de Ancoragem – Influência de Borda, Comprimento de Aderência, Posição e Orientação do Pino, Goiânia, 2005, Dissertação (mestrado) – Escola de Engenharia Civil, Universidade Federal de Goiás, 168 p.

Table 7 – Influence of anchor orientation

h_{ef} (mm)	Casting position	A_n/A_0	Horizontal: Specimen	Horizontal: $F_{u,H.}$ (kN)	Vertical: Specimen	Vertical: $F_{u,V.}$ (kN)	$F_{u,H.}/F_{u,V.}$
50	Top	1.0	P01	29.5	P06	28.4	1.04
		0.9	P02	21.6	P07	22.4	0.96
		0.8	P03A	21.5	P08B	23.0	0.93
		0.7	P04	16.4	P09B	17.0	0.96
	Bottom	1.0	P22	37.0	P27	40.6	0.91
		0.9	P23	33.0	P28	32.7	1.01
		0.8	P24	26.8	P29	24.8	1.08
		0.7	P25	22.1	P30A	22.4	0.99

Value	$F_{u,H.}/F_{u,V.}$
Maximum	1.08
Minimum	0.91
Mean	0.99
Coeff. of variation (%)	5.6

Figure 6 – Vertical displacement D4 in anchor bar axis in relation to concrete block

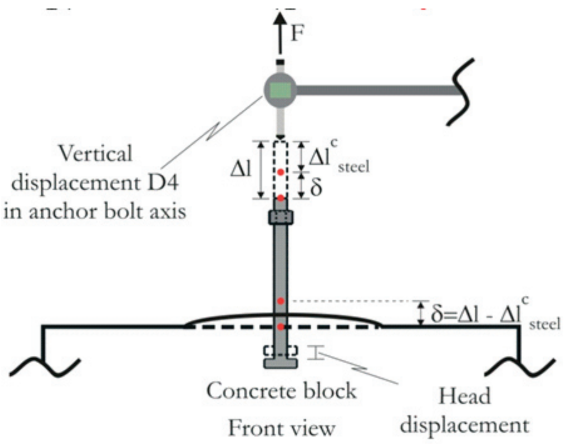

Figure 7 – Percentage of failure load (F_u) versus displacement δ curves, for embedment depth of 50 mm and 100 mm at different casting positions

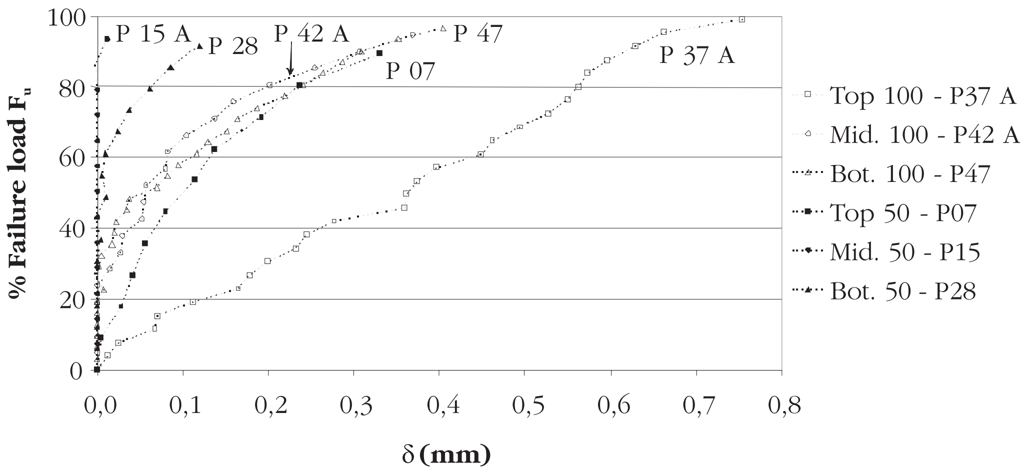

Figure 8 – Percentage of failure load (F_u) versus displacement δ curves, for embedment depth of 50 mm and 100 mm with and without bond